Aerodynamic Optimization using Navier-Stokes Equations and Continuous or Discrete Adjoint Formulation

S.Hiernaux*, J.A. Essers†

Abstract

In this paper, a method based on the optimal control theory for the resolution of shape optimization problems in aerodynamics is presented. This method permits a faster computation of the gradients used in classical optimization algorithms, such as the descent methods. The theoretical results given by optimal control theory are first recalled and then applied to the 2D Euler and Navier-Stokes equations, using two different approaches, one based on the equations in their analytical form, and the other based on the discrete equations. The algorithms of resolution of the state and adjoint equations, and the optimization procedure are then described. Some results obtained on inviscid test cases are presented, as well as some preliminary results on viscous test-cases

1 Introduction

Since the last decade, due to the spectacular progress in the computer science, the Computational Fluid Dynamics has strongly evolved: simulation of highly complex, three-dimensional and turbulent flows is now a common task.

With the capacity of today's computers, one can envisage the resolution of shape optimization problems. Nevertheless, optimization methods require many evaluations of different aerodynamic configurations, and so are much more expensive than a single analysis. It is therefore mandatory to find methods that evaluate aerodynamic functions and their gradient at the lowest possible computational cost.

Classical optimization techniques (descent methods) not only require the value of the function to optimize, but also of its gradient. The classical way to compute the gradient is to use a finite-difference formula; the main drawback of this method is due to the fact that $n+1$ evaluations of aerodynamic functions are necessary, n being the number of parameters defining the geometry to optimize. So, such methods are completely unsuited to aerodynamic shape optimization, due to the high computational cost of the single analysis.

In this paper, a method based on optimal control theory (see [1],[6],[7]) to evaluate the gradient is presented. The computational cost of this method is approximatively the same as the evaluation of the aerodynamic function, regardless of the number of design parameters, and is well adapted to shape design problems.

Our present results are quasi-unconstrained inviscid problems solved by a quasi-Newton algorithm. At the time of the conference, we intend to presents viscous problems using Navier-Stokes equations, with non-linear constraints. The optimizer should be a convex linearization program developed at the University of Liege.

*Research Assistant,Aerodynamics group, University of Liege

†Professor, Aerodynamics group, University of Liege

2 Optimal control theory for shape design optimization

The shape optimization problem considered here have the form:

$$\text{minimize}_{\Sigma_d} \mathcal{F}(\mathbf{s}(\mathbf{u}), \mathbf{u}) \tag{1}$$

where Σ_d is the surface whose shape has to be optimized, $\mathbf{u}$ the design variables and $\mathbf{s}$ are the state variables given over the domain Ω by the PDE:

$$L[\mathbf{s}, \mathbf{u}] = 0 \tag{2}$$

with the boundary conditions: $\mathbf{G}_i(\mathbf{s}) = 0$

The optimality condition (see [3]) states that the *Lagrangian*

$$\mathcal{L} = \mathcal{F} + < \psi, L[\mathbf{s}, \mathbf{u}] >_\Omega + \sum_i < \mu_i, \mathbf{G}_i >_{\Sigma_i} \tag{3}$$

(where ψ, μ_i respectively defined on the domain and on the boundaries are the costate variables) is *stationnary*, i.e. $\delta\mathcal{L} = 0$ for any admissible arbitrary variation $\delta\mathbf{u}, \delta\mathbf{s}, \delta\psi, \delta\mu_i$ of the design, state and costate variables. The notation $< f, g >$ denotes a scalar product.

The variation of $\mathcal{L}$ due to variations in ψ and μ_i is zero if the state equations and boundary conditions are satisfied. The variation of $\mathcal{L}$ due to variations in $\mathbf{s}$ is:

$$\begin{aligned} \delta\mathcal{L}_\mathbf{s} &= \partial_\mathbf{s}\mathcal{F}\delta\mathbf{s} + < \psi, L[\delta\mathbf{s}] >_\Omega \\ &+ \sum_i < \mu_i, \partial_\mathbf{s}\mathbf{G}_i\delta\mathbf{s} >_{\Sigma_i} \end{aligned} \tag{4}$$

The integral on Ω in the expression above can be worked out with the gauss formula to give:

$$\begin{aligned} \delta\mathcal{L}_\mathbf{s} &= \partial_\mathbf{s}\mathcal{F}\delta\mathbf{s} + \sum_i < L_n^T\psi, \delta\mathbf{s} >_{\Sigma_i} \\ &- < L^T[\psi], \delta\mathbf{s} > \\ &+ \sum_i < \mu_i, \partial_\mathbf{s}\mathbf{G}_i\delta\mathbf{s} >_{\Sigma_i} \end{aligned} \tag{5}$$

where L_n is the spatial operator projected on the boundaries. For example, if the spatial operator $L[\mathbf{s}]$ has the form

$$\partial_x\mathbf{f}(\mathbf{s}) + \partial_y g\mathbf{s})$$

then the projected spatial operator is

$$\mathbf{f}n_x + \mathbf{g}n_y$$

with n_x, n_y the components of the normal to the surface.

Assuming that $\mathcal{F}$ has the form $\mathcal{F} =< 1, \Phi(\mathbf{s}) >$, then the lagrangian $\mathcal{L}$ is stationary with respect to variations of $\mathbf{s}$ if the following costate (or adjoint) equations and boundary conditions are verified:

$$L^T[\psi] = 0 \quad \text{in } \Omega \tag{6}$$

$$L_n^T\psi = \partial_\mathbf{s}\mathcal{H} \quad \text{on } \Sigma \tag{7}$$

where the Hamiltonian $\mathcal{H}$ is defined as

$$\begin{aligned} \mathcal{H} &= \Phi + \mathbf{G}_d^T\mu_d \quad \text{on } \Sigma_d \\ \mathcal{H} &= \mathbf{G}_i^T\mu_i \quad \text{on } \Sigma_i \end{aligned}$$

The variation of $\mathcal{L}$ due to variations of the design variables $\delta\mathbf{u}$ is zero when the *design equation* is verified:

$$\partial_\mathbf{u}\mathcal{F} + < \psi, \partial_\mathbf{u}L[\mathbf{s}] >= 0 \tag{8}$$

This equation is used to build the gradient used in the classical descent optimization algorithms.

3 Continuous adjoint formulation applied to Navier-Stokes equations

3.1 The Navier-Stokes equations

The 2D Navier-Stokes Equations have the form:

$$\partial_x(\mathbf{f}-\mathbf{f}_v)+\partial_y(\mathbf{g}-\mathbf{g}_v)=0 \tag{9}$$

where $\mathbf{f},\mathbf{g}$ are the inviscid fluxes, function of the state variables $[\rho,\rho u,\rho v,\rho E]^T$:

- $\mathbf{f}=\left[\rho u,p+\rho u^2,\rho uv,\rho uH\right]^T$;
- $\mathbf{g}=\left[\rho v,\rho uv,p+\rho v^2,\rho vH\right]^T$

with

- ρ is the density, u,v the two components of the velocity, E the internal energy per unit mass;
- $p=(\gamma-1)\left(\rho E-\frac{1}{2}\rho(u^2+v^2)\right)$ is the pressure;
- $H=\gamma E-\frac{\gamma-1}{2}\left(u^2+v^2\right)$ is the internal enthalpy per unit mass;
- $\gamma=\frac{c_p}{c_v}$ is the ratio of the specific heats.

The viscous fluxes have the form:

- $\mathbf{f}_v=[0,\tau_{xx},\tau_{xy},u\tau_{xx}+v\tau_{xy}-q_x]^T$
- $\mathbf{g}_v=[0,\tau_{xy},\tau_{yy},u\tau_{xy}+v\tau_{yy}-q_y]^T$

The components of the stress tensor τ and the thermal flux $\vec{q}$ can be expressed in term of the first derivative of the primitive variables $[\rho,u,v,T]^T$:

- $\tau_{xx}=\frac{4}{3}\mu\partial_x u-\frac{2}{3}\mu\partial_y v$
- $\tau_{yy}=\frac{4}{3}\mu\partial_y v-\frac{2}{3}\mu\partial_x u$
- $\tau_{xy}=\mu\left(\partial_y u+\partial_x v\right)$
- $\vec{q}=-k\vec{\nabla}T$

with $\mu(T)$ the dynamic viscosity, and $k(T)$ the thermal conductivity.

The following boundary conditions are applied:

- subsonic inlet: the total pressure, the Mach number and the flow direction are imposed;
- supersonic inlet: the state vector $\mathbf{s}$ is imposed;
- subsonic outlet: the pressure p is imposed;
- supersonic outlet: no condition;
- slip wall:
$$u_n=un_x+vn_y=0 \tag{10}$$
where $\mathbf{n}=(n_x,n_y)$ is the normal to the wall.
- viscous wall:
  - the no-slip condition: $u=v=0$
  - the isothermal condition $T=T_0$ or adiabatic condition $\vec{\nabla}T\cdot\vec{n}=0$

3.2 Optimization problem

The functional to minimize has the form:

$$\mathcal{J}=\int_{\Gamma_f}\Phi(p,\tau_w)d\Gamma_f \tag{11}$$

with p the pressure and

$$\tau_w=\mu\frac{\partial u_s}{\partial n}$$

the wall shear stress. u_s is the tangential component of speed.

3.3 Adjoint equations and boundary conditions

The adjoint equations and boundary conditions are obtained by stating that the variation of the*Lagrangian*:

$$\mathcal{L} = \int_{\Gamma_f} \Phi(p, \tau_w) d\Gamma_f - \int_\Omega \psi^T \left(\partial_x(\mathbf{f} - \mathbf{f}_v) + \partial_y(\mathbf{g} - \mathbf{g}_v)\right) d\Omega + \sum_i \int_{\Gamma_i} \mu_i^T \mathbf{G}_i d\Gamma_i \tag{12}$$

with respect to the state variables $\mathbf{s}$ is stationary, i.e.:

$$\begin{aligned} \delta\mathcal{L}_\mathbf{s} &= \int_{\Gamma_f} \frac{\partial\Phi}{\partial p}\tilde{p} + \frac{\partial\Phi}{\partial\tau_w}\tilde{\tau}_w \, d\Gamma_f \\ &- \int_\Omega \psi^T \left(\partial_x(\tilde{\mathbf{f}} - \tilde{\mathbf{f}}_v) + \partial_y(\tilde{\mathbf{g}} - \tilde{\mathbf{g}}_v)\right) d\Omega \\ &+ \sum_i \int \Gamma_i \mu_i^T \tilde{\mathbf{G}}_i d\Gamma_i = 0 \end{aligned} \tag{13}$$

where $\tilde{(.)}$ represents the variation of the quantity $(.)$ due to the variation of $\mathbf{s}$.

The term over the domain can be splitted into inviscid and viscous variations:

$$\int_\Omega \psi^T \left(\partial_x(\tilde{\mathbf{f}} - \tilde{\mathbf{f}}_v) + \partial_y(\tilde{\mathbf{g}} - \tilde{\mathbf{g}}_v)\right) d\Omega = \delta\mathcal{I} - \delta\mathcal{V}$$

with:

$$\delta\mathcal{I} = \int_\Omega \psi^T \left(\partial_x\tilde{\mathbf{f}} + \partial_y\tilde{\mathbf{g}}\right) d\Omega \tag{14}$$

$$\delta\mathcal{V} = \int_\Omega \psi^T \left(\partial_x\tilde{\mathbf{f}}_v + \partial_y\tilde{\mathbf{g}}_v\right) d\Omega \tag{15}$$

3.3.1 Inviscid part

The inviscid variation (14) can be worked out by Gauss formula to give:

$$\delta\mathcal{I} = \sum_i \int_{\Gamma_i} \psi^T \tilde{\mathbf{f}}_n d\Gamma_i - \int_\Omega \left(\mathbf{A}^T\partial_x\psi + \mathbf{B}^T\partial_y\psi\right)^T \delta\mathbf{s} d\Omega \tag{16}$$

where $\mathbf{A}, \mathbf{B}, \mathbf{f}_n$ are the same as for the Euler equations.

Applying no-slip boundary conditions, one finds that

$$\psi^T\tilde{\mathbf{f}}_n = \psi_n\tilde{p} + \rho\left(\psi_1 + H\psi_4\right)\tilde{u}_n$$

on a viscous wall.

3.3.2 Viscous part

In order to simplify the calculation, it is assumed that the viscous variation vanishes on the outer boundaries and that the variation of the viscosity and thermal conductivity are small enough, and can be neglected. Applying Gauss formula on (15) leads to:

$$\delta\mathcal{V} = \int_{\Gamma_f} \psi^T \left(\tilde{\mathbf{f}}_v n_x + \tilde{\mathbf{g}}_v n_y\right) d\Gamma_f - \int_\Omega \tilde{\mathbf{f}}_v^T\partial_x\psi + \tilde{\mathbf{g}}_v^T\partial_y\psi d\Omega \tag{17}$$

After lengthy computation that can be found in [9], the viscous variation is finally:

$$\delta\mathcal{V} = \int_{\Gamma_f} \left[\psi_n\right]\tilde{\tau}_n + \left[\psi_s\right]\tilde{\tau}_w$$

$$
\begin{aligned}
&+\left[-\frac{2}{3}\mu\vec{\nabla}\cdot\vec{\psi}+2\mu\partial_n\psi_n-\mu\partial_s\psi_s-\frac{2}{3}\mu\frac{1}{R}\psi_n\right]\tilde{u}_n\\
&+\left[\mu\left(\frac{5}{3}\partial_s\psi_n+\partial_n\psi_s-\frac{2}{R}\psi_s\right)+\psi_4\tau_w\right]\tilde{u}_s\\
&-\left[k\psi_4\right]\vec{\nabla}\tilde{T}\cdot\vec{n}+\left[k\vec{\nabla}\psi_4\cdot\vec{n}\right]\tilde{T}d\Gamma_f\\
&+\int_\Omega\left[\partial_x\left(\Gamma_{xx}+\Lambda_{xx}\right)+\partial_y\left(\Gamma_{xy}+\Lambda_{xy}\right)-\tau_{xx}\partial_x\psi_4-\tau_{xy}\partial_y\psi_4\right]\tilde{u}\\
&+\left[\partial_x\left(\Gamma_{xy}+\Lambda_{xy}\right)+\partial_y\left(\Gamma_{yy}+\Lambda_{yy}\right)-\tau_{xy}\partial_x\psi_4-\tau_{yy}\partial_y\psi_4\right]\tilde{v}\\
&+\vec{\nabla}\cdot\left(k\vec{\nabla}\psi_4\right)\tilde{T}d\Omega
\end{aligned}
\tag{18}
$$

where R is the curvature radius of the surface Γ_f, and:

$$
\begin{aligned}
\Gamma_{xx} &= \frac{4}{3}\mu\partial_x\psi 2-\frac{2}{3}\mu\partial_y\psi_3 &(19)\\
\Gamma_{yy} &= \frac{4}{3}\mu\partial_y\psi 3-\frac{2}{3}\mu\partial_x\psi_2 &(20)\\
\Gamma_{xy} &= \mu\left(\partial_x\psi_3+\partial_y\psi_2\right) &(21)\\
\Lambda_{xx} &= \frac{4}{3}\mu u\partial_x\psi_4-\frac{2}{3}\mu v\partial_y\psi_4 &(22)\\
\Lambda_{yy} &= \frac{4}{3}\mu v\partial_y\psi_4-\frac{2}{3}\mu u\partial_x\psi_4 &(23)\\
\Lambda_{xy} &= \mu\left(u\partial_x\psi_4+v\partial_y\psi_4\right) &(24)
\end{aligned}
$$

The subscripts s, n refers to the tangential and normal-to-the-surface components.
The term on Ω can be written:

$$\int_\Omega \mathbf{h}^T\delta\mathbf{Q}d\Omega$$

with $\delta\mathbf{Q}=\left[\tilde{\rho},\tilde{u},\tilde{v},\tilde{T}\right]^T$ is the variation of the primitive variables. This variationis related to the variation of the conservative variables $\delta\mathbf{s}$ by the relation:

$$\delta\mathbf{Q}=\frac{\partial\mathbf{Q}}{\partial\mathbf{s}}\delta\mathbf{s}$$

with the Jacobian matrix:

$$
\frac{\partial\mathbf{Q}}{\partial\mathbf{s}}=\begin{pmatrix}
1 & 0 & 0 & 0\\
-\frac{u}{\rho} & 1 & 0 & 0\\
-\frac{v}{\rho} & 0 & 1 & 0\\
-\frac{\gamma}{\rho}\left(\frac{T}{\gamma}-\frac{1}{2}(u^2+v^2)\right) & -\frac{u\gamma}{\rho} & -\frac{v\gamma}{\rho} & \frac{\gamma}{\rho}
\end{pmatrix}
$$

The term on Ω is then equivalent to:

$$\int_\Omega \mathbf{h}'^T\delta\mathbf{s}d\Omega$$

with

$$\mathbf{h}'=\left(\frac{\partial\mathbf{Q}}{\partial\mathbf{s}}\right)^T\mathbf{h}$$

3.3.3 Contribution of the far-field boundary conditions

The contribution of the far-field boundary conditions on the variation of the Laplacian is:

$$\sum_i\int_{\Gamma_i}\mu_i^T\frac{\partial\mathbf{G}_i}{\partial\mathbf{s}}\delta\mathbf{s}d\Gamma_i \tag{25}$$

3.3.4 Contribution of the wall boundary conditions

The contribution of the wall boundary conditions on the variation of the Lagrangian is:

- for isothermal boundary conditions:

$$\int_{\Gamma_f} \mu_1 \tilde{u}_n + \mu_2 \tilde{u}_s + \mu_3 \tilde{T} d\Gamma_f \tag{26}$$

- for adiabatic boundary conditions:

$$\int_{\Gamma_f} \mu_1 \tilde{u}_n + \mu_2 \tilde{u}_s + \mu_3 \vec{\nabla} T \cdot \vec{n} d\Gamma_f \tag{27}$$

3.3.5 Contribution of the functionnal

The contribution of the functional is:

$$\int_{\Gamma_f} \frac{\partial \Phi}{\partial p} \tilde{p} + \frac{\partial \Phi}{\partial \tau_w} \tilde{\tau}_w \, d\Gamma_f \tag{28}$$

3.3.6 Adjoint equations

The adjoint equations are obtained by stating that the variation of the domain term of the Lagrangian is zero. Collecting terms in $\delta \mathbf{s}$ in the above variations, one finds:

$$\mathbf{A}^T \partial_x \psi + \mathbf{B}^T \partial_y \psi + \mathbf{h}^{'} = 0 \quad \text{ on } \Omega \tag{29}$$

The adjoint equations for inviscid (Euler) flows are obtained by dropping the term $\mathbf{h}'$ is the above expression.

3.3.7 Far-field adjoint boundary conditions

The far-field adjoint boundary conditions are obtained by cancelling term in $\delta \mathbf{s}$ in the contribution of the far-field boundary conditions:

$$\mathbf{A}_n^T \psi = \left(\frac{\partial \mathbf{G}_i}{\partial \mathbf{s}} \right)^T \mu_i \tag{30}$$

When dealing with inviscid wall, the above equation is applied

3.3.8 Adjoint boundary conditions on a viscous wall

Adjoint boundary conditions on a wall are obtained by cancelling the variation on Γ_f.

- Terms in $\tilde{\tau}_w$:

$$\frac{\partial \Phi}{\partial \tau_w} = -\psi_s \tag{31}$$

- Terms in $\tilde{u}_n$:

$$\mu_1 = \rho \left(\psi_1 + H \psi_4 \right) + \frac{2}{3} \mu \left(\vec{\nabla} \cdot \vec{\psi} + \frac{\psi_n}{R} \right) + \mu \partial_s \psi_s - 2 \mu \partial_n \psi_n \tag{32}$$

- Terms in $\tilde{u}_s$:

$$\mu_2 = -\tau_w \psi_4 - \mu \left(\frac{5}{3} \partial_s \psi_n + \partial_n \psi_s - \frac{2}{R} \psi_s \right) \tag{33}$$

- Terms in $\tilde{T}$:

$$\mu_3 = -k\vec{\nabla}\psi_4 \cdot \vec{n} \quad \text{if isothermal BC} \tag{34}$$

$$\vec{\nabla}\psi_4 \cdot \vec{n} = 0 \quad \text{if adiabatic BC} \tag{35}$$

- Terms in $\vec{\nabla}\tilde{T} \cdot \vec{n}$:

$$\psi_4 = 0 \quad \text{if isothermal BC} \tag{36}$$

$$\mu_3 = k\psi_4 \quad \text{if adiabatic BC} \tag{37}$$

- Terms in $\tilde{p}$:

$$\frac{\partial \Phi}{\partial p} = \psi_n \tag{38}$$

- Terms in $\tilde{\tau}_n$:

$$\psi_n = 0 \tag{39}$$

The last two boundary conditions are in conflict, so the functional Φ must be chosen as a $\Phi(p, \tau_w, \tau_n)$. Boundary condition (39) becomes:

$$\psi_n = -\frac{\partial \Phi}{\partial \tau_n} \tag{40}$$

which is compatible with (38) if:

$$-\frac{\partial \Phi}{\partial \tau_n} = \frac{\partial \Phi}{\partial p} \tag{41}$$

4 Discrete adjoint formulation

Generally, the continuous equations used in fluid dynamic are discretized to be solved numerically. The optimality conditions derived from the continuous equations may not be consistent with the numerical procedure used to solve the discrete equations. It may be therefore important to derive the adjoint equations from the discretized equations.

Consider the following problem:

$$\min F\left(\mathbf{u}, \mathbf{X}(\mathbf{u}), \mathbf{s}\left(\mathbf{X}, \mathbf{u}\right)\right) \tag{42}$$

under the constraints (discretized equations):

$$\mathbf{R}_i(\mathbf{X}, \mathbf{s}) = 0 \tag{43}$$

with $\mathbf{u}$ the control, $\mathbf{s}$ the state variables, $\mathbf{X}$ a vector defining the mesh used to discretize the space.

The necessary optimality condition is that the Laplacian:

$$\mathcal{L}(\mathbf{u}, \mathbf{s}, \psi) = F(\mathbf{u}, \mathbf{s}, \mathbf{X}(\mathbf{u})) - \sum_i \psi_i^T \mathbf{R}_i(\mathbf{X}(\mathbf{u}), \mathbf{s})$$

is stationary, i.e. the following equations are valid:

$$\text{State equations:} \quad \frac{\partial \mathcal{L}}{\partial \psi} = \mathbf{R}_i = 0 \tag{44}$$

$$\text{Adjoint equations:} \quad \frac{\partial \mathcal{L}}{\partial \mathbf{s}} = \frac{\partial F}{\partial \mathbf{s}} - \sum_i \psi^T \frac{\partial \mathbf{R}_i}{\partial \mathbf{s}} = 0 \tag{45}$$

$$\text{Design equation:} \quad \frac{\partial \mathcal{L}}{\partial \mathbf{u}} = \frac{\partial F}{\partial \mathbf{u}} + \frac{\partial F}{\partial \mathbf{X}}\frac{\partial \mathbf{X}}{\partial \mathbf{u}} - \sum_i \psi^T \left(\frac{\partial \mathbf{R}_i}{\partial \mathbf{X}}\frac{\partial \mathbf{X}}{\partial \mathbf{u}}\right) = 0 \tag{46}$$

5 Discretization and numerical solution

The optimality condition is composed of three equations (state,adjoint and design). Each of them can be viewed as an hypersurface in the space $\mathbf{s}, \psi, \mathbf{u}$. The numerical procedure must lead us to the intersection of these surfaces.

The most common method, which is the one used in this work, is to stand on the intersection of the state and adjoint surfaces, i.e. to have state and adjoint variables that satisfy state and adjoint equations, and to march to the design surface . This method is the well-known descent method, commonly used in mechanical optimization.

5.1 The Navier-Stokes equations

The Navier-Stokes equations (9) are discretized by finite-volume method and solved by an implicit time marching method. We refer the reader to [2] or [5] for more details.

Integrating the unsteady equations on a finite volume Ω_i and using the Gauss theorem yields:

$$\partial_t \int_{\Omega_i} \mathbf{s}\, d\Omega_i + \oint_{\Gamma} (\mathbf{F}(\mathbf{s},\mathbf{n}) - \mathbf{F}_v(\mathbf{s},\mathbf{n})\, d\Gamma \tag{47}$$

where $\mathbf{F} = \mathbf{f}n_x + \mathbf{g}n_y$ is the normal flux through the boundary Γ of the cell.

Considering polygonal cells, and integrating the flux using an n_g-points Gauss formula, gives:

$$\partial_t \int_{\Omega_i} \mathbf{s}\, d\Omega_i + \sum_{j \in N_i} l_j \sum^{n_g} w_g \left(\tilde{\mathbf{F}}_j - \tilde{\mathbf{F}}_{vj}\right) = 0 \tag{48}$$

where l_j is the length of the edge j, w_g the weight of the Gauss point,and N_i is the set of edges defining the control volume Ω_i. The numerical inviscid flux are computed using the Roe flux-difference splitting:

$$\tilde{\mathbf{F}} = \frac{1}{2}\left[\mathbf{F}(\mathbf{s}^L,\mathbf{n}) + \mathbf{F}(\mathbf{s}^R,\mathbf{n}) - |\tilde{\Omega}(\mathbf{s}^L,\mathbf{s}^R,\mathbf{n})|\left(\mathbf{s}^R - \mathbf{s}^L\right)\right] \tag{49}$$

where $\tilde{\Omega}$ is the Jacobian matrix evaluated using Roe's average of $\mathbf{s}^R, \mathbf{s}^L$, the latter being the value at the right or the left of the edges extrapolated from the center of the adjacent cells. This reconstruction can be of order 0 (constant), 1 (linear) or 2 (quadratic), and may imply complex detector-limiter to deal with flow discontinuities (shocks or slip lines).

A centered discretization is used to discretize the viscous terms of the Navier-Stokes equations. The viscous flux is evaluated at one point located at middle edge.

Once the spatial part is discretized, the equation is integrated in time with a fully implicit Newton-like method. At each time step, one must solve the following non-linear equation:

$$\mathcal{F}(\mathbf{s}^{n+1},\mathbf{s}^n) = \frac{\mathbf{s}^{n+1} - \mathbf{s}^n}{\Delta t} + \mathcal{R}(\mathbf{s}^{n+1}) = 0 \tag{50}$$

If this equation is linearized, we obtain the following linear system:

$$\left(\frac{\mathbf{I}}{\Delta t} + \mathcal{J}\right)\mathbf{s}^{n+1} = -\mathcal{F}(\mathbf{s}^n,\mathbf{s}^n) \tag{51}$$

with $\mathcal{J} = \frac{\partial \mathcal{R}}{\partial \mathbf{s}}$, the jacobian matrix. This system is solved by a 1-step Newton method using a ILU0 preconditioned GMRES Algorithm.

5.2 The continuous adjoint equations

The continuous adjoint equations (6) are discretized with the same finite-volume method as the Euler equations: the spatial part can be written as:

$$\mathcal{R}_i = \sum_{j \in N_i} l_j \sum^{n_g} w_g \tilde{\mathbf{G}}_j \tag{52}$$

with the numerical flux $\tilde{\mathbf{G}}_j$ is computed with a Roe-like flux splitting formula:

$$\tilde{\mathbf{G}} = \frac{1}{2}\left[\left(\mathbf{A}_n^T(\mathbf{s}^L)\psi^L + \mathbf{A}_n^T(\mathbf{s}^R)\psi^R\right) - |\tilde{\Omega}|^T\left(\psi^R - \psi^L\right)\right] \tag{53}$$

with $\mathbf{A}_n = \mathbf{A}n_x + \mathbf{B}n_y$. As for the state variables, the adjoint variables on the edges are extrapolated from the nodal values using a constant, linear, or quadratic reconstruction. The viscous term $\mathbf{h}$ is evaluated on the same point as the viscous flux of the Navier-Stokes equations.

The time integration is performed using the same method as for the Euler equations, i.e. fully-implicit Newton-like integration.

5.3 The discrete adjoint equations

The discrete adjoint equations (45) can be written:

$$\mathcal{J}^T\psi = -\frac{\partial F}{\partial \mathbf{s}} \tag{54}$$

with $\mathcal{J}_{ij} = \frac{\partial \mathbf{R}_i}{\partial \mathbf{s}_j}$ the jacobian matrix which is the same as the one used to solve the Euler equations by pseudo-time implicit methods.

This equation is solved by a totally implicit pseudo-time method, similar to the one used to solve the Euler equations:

$$\frac{\psi^{n+1} - \psi^n}{\Delta t} + \mathcal{J}^T\psi^n = -\frac{\partial F}{\partial \mathbf{s}} \tag{55}$$

5.4 The design equations: descent methods

If state, costate and design variables are known at iteration n, these variables are updated at the next step following the scheme:

$$\mathbf{u}^{n+1} = \mathbf{u}^n - \lambda\mathcal{G}(\mathbf{s}^n, \mathbf{u}^n, \psi^n) \tag{56}$$

$$L[\mathbf{s}^{n+1}, \mathbf{u}^{n+1}] = 0 \tag{57}$$

$$\partial_{\mathbf{s}}\mathcal{J}^{n+1} + < \psi^{n+1}, \partial_{\mathbf{s}}L >= 0 \tag{58}$$

where λ is a sufficently small scalar and

$$\mathcal{G} = \partial_{\mathbf{u}}\mathcal{J} + < \psi, \partial_{\mathbf{u}}L > \tag{59}$$

is a search direction.

The equation (56) is the updating step, and equations (57) and (58) simply means that the state and costate equations must be satisfied once the design variables are known.

If λ is small and equation (57) is satisfied, then:

$$L[\mathbf{s}^{n+1}, \mathbf{u}^{n+1}] = L[\mathbf{s}^n, \mathbf{u}^n] + \partial_{\mathbf{u}}L\delta\mathbf{u} + \partial_{\mathbf{s}}L\delta\mathbf{s} = 0 \tag{60}$$

and since $L[\mathbf{s}^n, \mathbf{u}^n] = 0$,

$$\delta\mathbf{s} = -\left[\partial_{\mathbf{s}}L\right]^{-1}\partial_{\mathbf{u}}L\delta\mathbf{u} \tag{61}$$

At step $n+1$ the functional can be writen:

$$\mathcal{J}^{n+1} = \mathcal{J}^n + \partial_{\mathbf{s}}\mathcal{J}\,\delta\mathbf{s} + \partial_{\mathbf{u}}\mathcal{J}\,\delta\mathbf{u} \tag{62}$$

or, taking into account (61),

$$\delta\mathcal{J} = \left[\partial_{\mathbf{u}}\mathcal{J} - \partial_{\mathbf{s}}\mathcal{J}\partial_{\mathbf{s}}L^{-1}\partial_{\mathbf{u}}L\right]\delta\mathbf{u} \tag{63}$$

with $\delta \mathbf{u} = \mathbf{u}^{n+1} - \mathbf{u}^n = -\lambda \mathcal{G}$. The variation of the functional is then:

$$\delta \mathcal{J} = -\lambda \left[\partial_{\mathbf{u}} \mathcal{J} - \partial_{\mathbf{s}} \mathcal{J} \partial_{\mathbf{s}} L^{-1} \partial_{\mathbf{u}} L \right] \left[\partial_{\mathbf{u}} \mathcal{J} + < \psi, \partial_{\mathbf{u}} L > \right] \tag{64}$$

If the costate variables ψ satisfy the costate equations (eq. (58) in stationary form, i.e. without the superscripts), then

$$\partial_{\mathbf{s}} \mathcal{J} \left[\partial_{\mathbf{s}} L \right]^{-1} = -\psi \tag{65}$$

and equation (64) becomes:

$$\begin{aligned} \delta \mathcal{J} &= -\lambda \left[\partial_{\mathbf{u}} \mathcal{J} + < \psi, \partial_{\mathbf{u}} L > \right] \left[\partial_{\mathbf{u}} \mathcal{J} + < \psi, \partial_{\mathbf{u}} L > \right] \\ &= -\lambda \left|| \mathcal{G} \right||^2 \leq 0 \end{aligned} \tag{66}$$

The direction $\mathcal{G}$ given by (59) is then a *descent direction* that can be used in the classical optimization algorithms.

The results presented in this paper are obtained with a quasi-Newton algorithm with BFGS update procedure, modified to take into account side constraints on the design variables.

At the time of the conference, test cases involving non-linear constraints will be presented. A linear convexification procedure [4] will be used to deal with such constraints.

6 Results

6.1 Airfoil parametrization

The initial airfoil section is a symmetric NACA0012. The profile is defined by the formula:

$$y(x) = y_c(x) + y_t(x) \tag{67}$$

where y_t and y_c are the thickness and camber distributions given by the following formula:

$$y_e(x) = \frac{t}{2} \left(\beta_1 \sqrt{x} + \sum_{k=2}^{6} \beta_k x^{k-1} \right) \tag{68}$$

$$y_c(x) = \begin{cases} \frac{c}{x_c^2} \left(-x^2 + 2 x x_c \right) & \text{if } x < x_c \\ \frac{c}{(1-x_c)^2} \left(-x^2 + 2 x x_c + 1 - 2 x_c \right) & \text{if } x > x_c \end{cases} \tag{69}$$

6.2 Adjoint variables for drag minimization of transsonic airfoil

The test case is drag minimization at M=0.8 and incidence of 2 degrees, with a low bound on the surface of the airfoil. In such a configuration, there is a shock on the lee-side of the airfoil. This discontinuity in the state variable induces Dirac peaks in the adjoint solution The first adjoint variable at the first iteration step is shown below.

This peak is smoothed by the numerical computation which involves a numerical dissipation scheme. Attempts to use a less diffusive flux (i.e. a Roe-type flux difference splitting) may lead to a failure of convergence.

This type of discontinuity is inherent to the problem, because the shock in the flow solution is not differentiable. Such Dirac discontinuities can be found also when using the flow sensibility derivatives to compute the gradient (see [8])

The optimization decreases the drag from 0.04968 to 0.01761 in about 30 iterations, see figure 2.a. The shape modification is shown on figure 2.b.

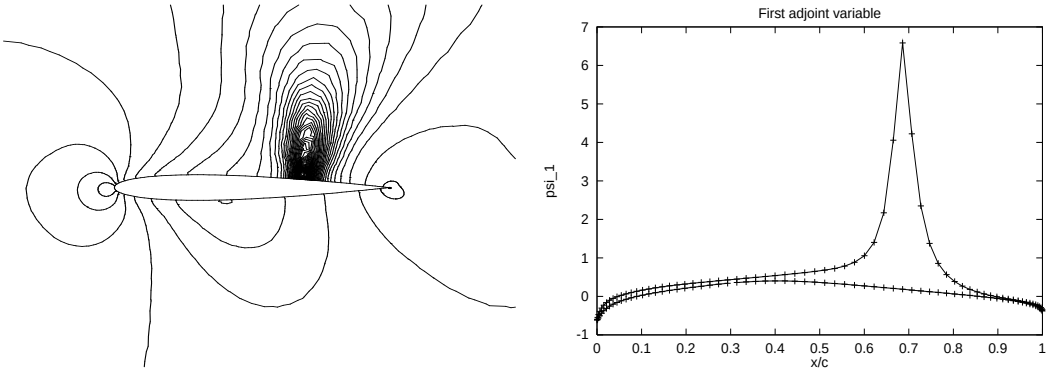

Figure 1: First adjoint variable

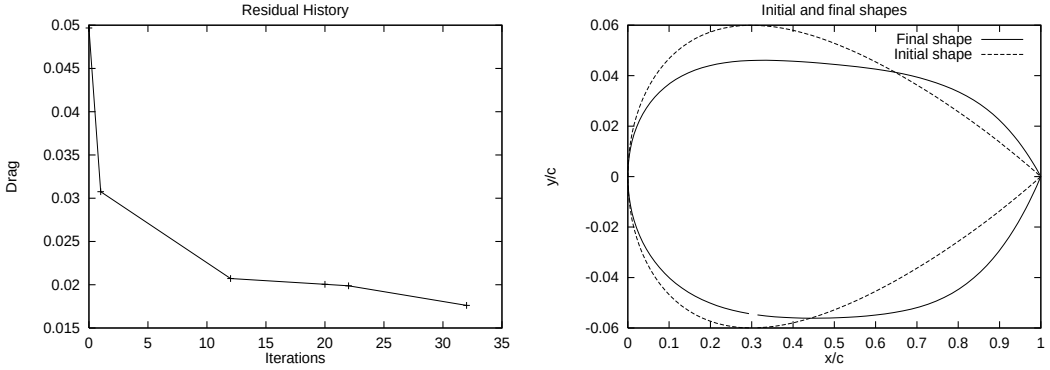

Figure 2: Residual history and shape modification

6.3 Transsonic Lift/Drag Ratio optimization

The problem of minimizing the ratio $\frac{C_d}{C_l}$ is not obvious because the cost function cannot be written in the form (11), although C_l and C_d have this form.

The gradient of $f = \frac{C_d}{C_d}$ is

$$\nabla f = \frac{1}{C_l} \left(\nabla C_d - f \nabla C_l \right) \tag{70}$$

One straightforward approach is to compute *two* adjoint problems, with functions C_l and C_d and to put their gradients in the formula above. Another method consist in using the functional $\tilde{f} = \frac{1}{C_{l_0}} \left(C_d - f_0 C_l \right)$, defined at the current design point α_0, for the computation of the gradient. This function has the same gradient as the initial cost function at the current design point, and has the form (11), because it is linear in C_l and C_d. Its gradient requires only *one* adjoint computation.

The optimization has been performed using the continuous and the discrete adjoint formulations. The residual histories and shape modifications for both computations are given on figure (3) below.

As can be seen from the figure above, the discrete approach allows a larger decrease of the function. This can be explained by the fact that the discrete formulation uses a gradient consistent with the numerical solution of the Euler equations.

6.4 Subsonic viscous flow

In this subsonic viscous case (M=0.5, Re=100000), the drag is mainly produced by the viscosity. The flow around the initial airfoil presents a circulation bubble that induce drag (see fig. 6). This circulation bubble can also be seen on the Skin friction coefficient plot (fig 5.b): it extends on the aft half of the succion side.

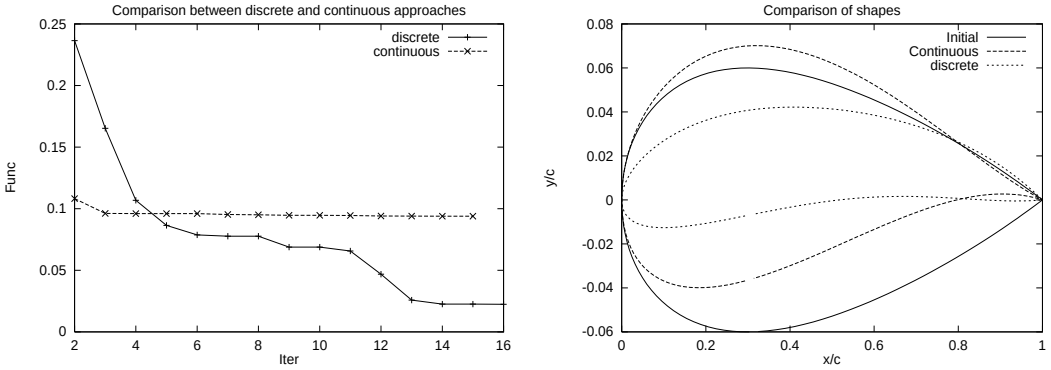

Figure 3: Residual history and shape modifications

After ten iterations, the drag coefficient has drop from 0.03649 to 0.02975. The final profil is shown on figure 4.b. The flow around optimized profile doesn't show any recirculation bubble, and the drag is lowered (see figures 6)

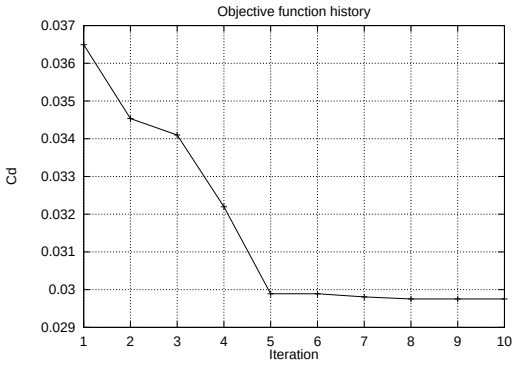

Figure 4.a: Convergence history

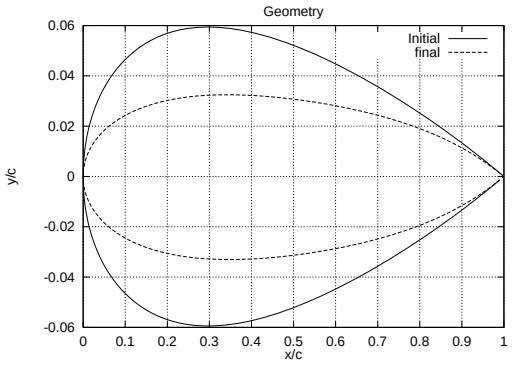

Figure 4.b: Comparison of geometries

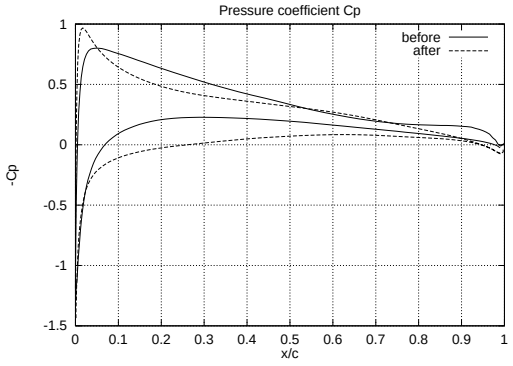

Figure 5.a: Cp comparison

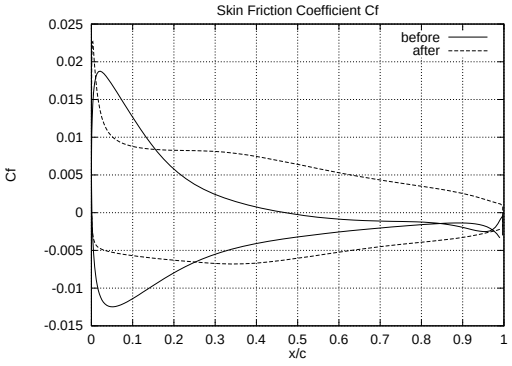

Figure 5.b: Cf comparison

7 Conclusions and prospects

In this abstract, we have presented a method to compute gradients required by shape optimization methods in CFD. This approach, based on optimal control theory, is much less

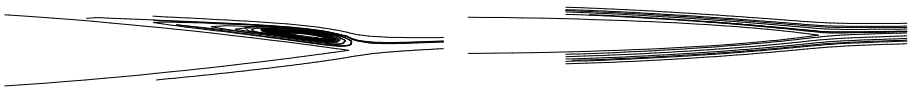

Figure 6: Streamlines on the aft part of initial (left) and final (right) airfoils

time-consuming than the classical finite-difference methods. Preliminary results show that the gradient conputed can be used in descent methods.

The following results will be presented at the conference :

- treatment of new problems: inverse design of airfoil (i.e. pressure matching problems), viscous flows
- comparison of the continuous-based and discrete-based adjoint method, in term of accuracy and effectiveness;
- new optimization algorithms: constrained problems solved by linear convexification;
- new airfoil parametrization involving Bezier curves.

References

[1] J. Reuther A. Jameson. Control Theory Based Airfoil Design using the Euler Equations. AIAA Report 94-4272-CP, American Institute for Aeronautics and Astronautics, 1994.

[2] M. Delanaye. *Polynomial Reconstruction Finite Volume Schemes for The Compressible Euler and Navier-Stokes Equations on Unstructured Adaptative Grids.* PhD thesis, Université de Liège, 1996.

[3] V.L. Syrmos F.L. Lewis. *Optimal control.* John Wiley and sons, 1995.

[4] L.A. Schmit H. Smaoui, C. Fleury. Advances in Dual Algorithms and Convex Approximation Methods. In *AIAA/ASME/ASCE/AHS 29th Structures, Structural Dynamics and Materials Conference, Williamsburg, VI*, 1988.

[5] C.H. Hirsch. *Numerical Computation of Internal and External Flows*, volume I and II. John Wiley and sons, 1990.

[6] A. Jameson. Aerodynamic Design via Control Theory. *Journal of Scientific Computing*, 3(3), 1988.

[7] A. Jameson. Optimum Aerodynamic Design via Boundary Control. AGARD Report R-803, AGARD-FDP-VKI Special Course at Von Kármán Institute, Apr. 1994.

[8] M.D. Gunzburger J.R. Appel. Difficulties in Sensitivity Calculations for Flows with Discontinuities. *AIAA Journal*, 35(5), May 1997.

[9] B. Soemarwoto. The Variational Method for Aerodynamic Optimization Using the Navier-Stokes Equations. ICASE Report 97-71, NASA Langley Research Center, Hampton, Virginia, 1997.